

## N O T I C E

THIS DOCUMENT HAS BEEN REPRODUCED FROM  
MICROFICHE. ALTHOUGH IT IS RECOGNIZED THAT  
CERTAIN PORTIONS ARE ILLEGIBLE, IT IS BEING RELEASED  
IN THE INTEREST OF MAKING AVAILABLE AS MUCH  
INFORMATION AS POSSIBLE

(NASA-CR-162766) THE INVESTIGATION OF TIME  
DEPENDENT FLAME STRUCTURE BY IONIZATION  
PROBES (Sheffield Univ.) 23 p HC A02/MF A01  
CSCL 21B

N80-17162

Unclas  
47169

G3/25

THE INVESTIGATION OF TIME DEPENDENT FLAME STRUCTURE  
BY IONISATION PROBES

by

J. M. P. Ventura, T. Suzuki, A. J. Yule, S. Ralph  
and N. A. Chigier\*

Department of Chemical Engineering and Fuel Technology,  
University of Sheffield, England

\* Author to whom correspondence should be sent:

Department of Chemical Engineering and Fuel Technology,  
University of Sheffield,  
Mappin Street,  
Sheffield S1 3JD, England

Subject Matter:

- (32) Turbulent Combustion
- (5) Fluid Dynamics
- (3) Experimental Methods

PROCESSED BY  
DATE: 2-26-80  
DCAF NO. 215000  
PROCESSED BY  
 NASA STI FACILITY  
 ESA - SDS  ARA

THE INVESTIGATION OF TIME DEPENDENT FLAME STRUCTURE  
BY IONISATION PROBES

by

J. M. P. Ventura, T. Suzuki, A. J. Yule, S. Ralph  
and N. A. Chigier

Abstract

In this study, ionisation probes have been used to measure mean ionisation current and frequency spectra, auto-correlations and cross-correlations in jet flames with variation in the initial Reynolds numbers and equivalence ratios. Special attention has been paid to the transitional region between the burner exit plane and the plane of onset of turbulence.

Evidence of a double vortex structure was found, with low velocity large vortices at the outer part of the mixing layer and smaller, faster moving vortices on the inner side. These vortices distort the reaction zone and can thus be detected by the ionisation probes. Systematic variations of mean ionisation level distributions and spectra were found with variation in both Reynolds number and equivalence ratio. The transition to turbulence is indicated by the axial variations of auto-correlations and frequency spectra. A double probe cross-correlation technique showed the loss of coherence of the initial vortices as they are convected downstream and it is also used to measure the convection velocities of the reacting interfaces associated with the vortices. The convective properties of the vortices are also found to be dependent on the initial Reynolds number and equivalence ratio of the flame. The large outer vortices, in the first 15 diameters of flow, are convected at lower velocities than the equivalent eddies in the cold jet, but they accelerate as they move downstream. The smaller, inner vortices move at approximately the local mean velocity. Laser anemometer measurements show that the jet potential core increases in length by a factor of 5 compared with

the cold jet core, for the flames studied. However, spectra indicate a lengthening of the transition region by a factor of 3. The usefulness of ionisation probes for the determination of flame structure is demonstrated and the combination of these high frequency response multiprobe techniques with statistical data analysis methods, gives a unique capability for the determination of a detailed description of the time dependent transitional and turbulent flame structure.

### Introduction

Mixing layers with chemical reaction have been studied very intensively in the last few years. One of the most important examples is the round free jet flame, in so far as it is the basic model for most of the burner systems being used in industrial furnaces and combustion chambers. The presence of coherent structures in jets (both in cold flow and flame situations) has now been clearly established. However, these structures are very often masked by a certain degree of randomness, so that their detection has to be carried out using statistical techniques such as correlations and frequency spectra measurements. The authors<sup>1</sup> have described an experimental investigation of coherent structures in jet flames and have given a general description of the vortex structures found in these flames. We describe, here, detailed time resolved measurements in a jet flame obtained by using ionisation probes, which have particular advantages of high frequency response and good spatial resolution.

The existence of positive ions in hydrocarbon flames has long been recognized, and mechanisms to explain their generation and recombination were proposed<sup>2</sup> and are now generally accepted. Because it decreases very sharply on both sides of a reaction zone due to the fast ion recombination, ion density can be used to detect the presence of flame. Karlovitz et al.<sup>3</sup> were the first to apply ionisation probes (essentially a wire, negatively biased to attract positive ions) for that purpose. Since then, they have been used by many workers;<sup>4, 5, 6</sup> a review<sup>7</sup> of the theories supporting the

use of this probe has been published recently.

In the present work the ionisation probes have been used to study the transitional region in turbulent flames. The decay of coherence has been studied; convection velocities and flow velocities are compared. A picture emerges according to which the flame characteristics are strongly influenced by the interfaces between the mixing layer and the outer flow on one side, and the potential core on the other side.

### Experimental Apparatus

The experimental set up has been described in detail previously,<sup>8</sup> so that only the principal characteristics will be presented here. It consists mainly of a round burner (diameter 25.4 mm) in the centre of a square nozzle (400 x 400 mm), which provides a secondary air stream with a mean velocity of  $0.8 \text{ ms}^{-1}$ . The burner tube is fed with a mixture of propane and air in various proportions. The secondary air stream provides some shielding of the flame from small draughts; but it is mainly intended as a means of seeding the outer side of the mixing layer for laser anemometry measurements. Experiment has shown that biasing in velocity measurements occurs when only one side of the mixing layer is seeded.

Turbulence levels in both the jet and surrounding exit streams are less than 1%. The whole burner assembly can be moved vertically and horizontally; furthermore, the probe holder is also movable, thus facilitating the complete mapping of the flame field. The ionisation probes used were similar to the ones reported by Suzuki et al.<sup>6</sup> Mean flow velocity was measured with a conventional small angle side scatter laser doppler anemometer, using a Spectra Physics 164 argon-ion laser at 800 mW, coupled with a Cambridge Consultants frequency tracker.

Other instrumentation used included a Hewlett-Packard 3721A Correlator to measure auto- and cross-correlations, and a Real Time Analyser Model SD 335, to measure frequency spectra.

## Results

Radial profiles of mean ion current and mean velocity in flames with the same equivalence ratio  $\phi = 2.62$  and Reynolds numbers  $Re = 5 \times 10^3$ ,  $10^4$  and  $1.5 \times 10^4$  are presented in Figure 1, for two different axial distances,  $x/D = 8$  and  $16$ .

As far as the mean ion current profiles are concerned, the peak value increases with Reynolds number at both axial stations. A similar trend with increasing  $Re$  has been described by Clements and Smy<sup>9</sup> for premixed flames. At  $x/D = 16$ , the profiles are wider and, in the case of the lowest  $Re$  flame, the maximum is located at the flame axis. This gives an indication of the width of the region where combustion takes place. The mean velocity profiles show the persistence of the jet potential core up to and beyond  $x = 16D$ . High velocity gradients are also found far downstream, at the inner side of the mixing layer. The occurrence of inflexion points and 'humps' in the velocity profiles is also seen.

Figure 2 shows typical traces of ion current signal obtained with two ionisation probes, placed 10 mm apart, at  $x/D = 8$  and  $16$ . The existence of a basically periodic signal in the upstream location contrasts strongly with the much more random signal at the downstream point. The difference between the smooth shape of the first signal and the 'spiky' appearance of the second is also to be noted. At each position the signals from the two probes are quite similar, although displaced in time. However, a more detailed comparison between the signals, at one station, indicates significant differences; for example the appearance or disappearance of peaks between the pair of probes and differences in the time delays between corresponding peaks. This indicates that one cannot make the simple assumption of a convected 'frozen' flow pattern even with such a relatively small probe separation of 10 mm.

Figure 3 presents normalized power spectra of ion current for two flames with the same Reynolds number ( $Re = 10^4$ ) but different equivalence ratios ( $\phi = 2.62$  and  $10.4$ ), obtained at axial distances  $x/D = 4$ ,  $12$  and  $16$

and at a radial distance  $r/D = 0.5$ . The main features of the spectra are similar in both flames; the presence of pronounced peaks at  $x/D = 4$  due to periodic vortex structures, a general smoothing of the spectra with increased downstream distance, and the final disappearance of any identifiable discrete frequency. The peaks are also clearer in the flame with the lower equivalence ratio.

Spectra in flames with  $\phi = 2.62$  and  $Re = 5 \times 10^3$ ,  $1.0 \times 10^4$  and  $1.5 \times 10^4$  have been measured at radial distance  $r/D = 0.5$  and axial distance  $x/D = 4$  (Fig. 4), to study variation of spectra with Reynolds number. It may be noted that discrete frequencies are very pronounced in all flames which is expected due to the proximity to the burner exit. Also, a small shift of the discrete frequencies with changing  $Re$  can be detected. The larger number of peaks noticeable in the lower Reynolds number flame do not correspond to the actual presence of different fluctuations, but rather are harmonics of the main frequency (the corresponding time signal had a shape roughly similar to a square wave).

A change in the higher frequency region of the spectra is evident, namely the appearance of sharp spikes with increasing Reynolds number; this is attributed to the fact that, with increasing exit velocity, the mixing layer's average radial location with respect to the jet flame centre line changes, so that, while the measurements are taken in a fixed position relative to the burner port, the locations are slightly different with respect to the mixing layer. The effect of this is that the signal may be more or less influenced by the higher frequency structure which is found at the inner interface of the mixing layer as described later and noted in ciné films previously described by the authors.<sup>1</sup> This influence will also be discussed in the light of cross-correlation measurements.

A set of auto-correlation measurements, obtained with an ionisation probe in a flame with  $\phi = 2.62$  and  $Re = 10^4$ , at distances downstream the nozzle between 4 and 12 diameters are presented in Figure 5. The strong periodicity in the signal is evident up to about 8 diameters downstream. After that, turbulence becomes established and the auto-correlation is of

the form generally found for a random signal.

This decay in the periodicity of the ionisation signals results from a decay in the periodicity and coherence of the vortices which interact with the reaction zone. The decay of the periodic auto-correlations is evident in Figure 6, where the ratio between the second and the main peaks in the auto-correlogram is plotted against normalized axial distance for two flames with the same Reynolds number ( $10^4$ ) and different equivalence ratio (2.62 and 10.4). It can be seen that the flame with the lower equivalence ratio retains coherence of the vortex structures until further downstream.

Cross-correlations between the signals from two ionisation probes, with separation of the sensing wires in the  $x$  direction, were obtained in two different ways; (a) a set of measurements was carried out keeping a fixed streamwise separation between probes (10 mm) and moving both probes relative to the burner exit; (b) another set of data was obtained keeping the upstream probe at a fixed position ( $x/D = 4$ ) and moving the second probe downstream.

From the cross-correlation curve, convection velocity was obtained by dividing the inter-probe distance by the delay time between the origin and the first positive peak. Applying this definition to the curves obtained by the two methods presented above, two different physical interpretations of convection velocity are derived: for a fixed inter-probe distance, the value obtained is a local value, which is more uniquely related to the measuring position, and less dependent on the energy content of the signal; for the second method (variable distance between probes), especially for the larger probe separation, convection velocity is more related to those structures which are able to maintain their identity for longer distances.

Figure 7 presents cross-correlograms obtained by using a pair of ionisation probes with varying streamwise separation. Besides the overall shape expected for this kind of measurement, there is a noticeable high frequency 'kink' at the beginning of the cross-correlograms (except for the smallest



inter-probe distance where the time resolution of the measurement is probably not enough for its detection). The physical interpretation of this small inflection point is based upon evidence<sup>1</sup> provided by Schlieren high speed ciné films, which clearly show the mixing layer to be bounded by two different interfaces: the inner one with a shorter wavelength instability and being convected downstream relatively faster; the outer interfaces more widely folded, with lower frequency and a lower convection velocity. The Schlieren technique and ionisation probes respond to two different aspects of the flame structure; the first technique is sensitive to density gradients while the ionisation probes are sensitive to ion density, thus closely detecting the presence of flame fronts. Therefore great care must be taken to compare results derived from these two different techniques. It is thought, nevertheless, that the small kink in the curves corresponds to smaller vortices being convected at higher velocities.

In Figure 8 data obtained from several flames are presented, where probe separation distance is plotted against delay time between the origin and the first positive main peak. The points are distributed in the graph in two clearly distinct groups; one set obtained from the small high frequency kinks present in cross-correlation curves for two different flames; and another set derived from the main peak of the cross-correlograms. This indicates that, for certain of the flames studied, the local mixing layer flame structure is simultaneously influenced by two sets of vortex motions at both interfaces. However, for other flames the oscillations on the outer interface (between the mixing layer and the secondary flow) are definitely the dominant influence. It is found that the convection velocities of the inner high frequency instability waves (or vortices), were approximately  $0.85 U_j$ , which agreed with the velocities of the inner vortices measured from ciné films.<sup>10</sup> Although convection velocities obtained from the fixed and variable interprobe distance methods have a somewhat different physical interpretation, the actual values obtained do not fall very far apart, as can be seen from

Figure 9, where data obtained from both methods are compared. This figure shows variation in convection velocity of the main correlation peak, with axial distance, along  $r/D = 0.5$ . The straight line is the least square fit to the measurements obtained with a fixed distance between probes.

Figure 10 presents a comparison of radial profiles of flow velocity obtained with laser anemometry and convection velocity derived from the cross-correlations between two probes, spaced 10 mm apart in the streamwise direction. Both profiles were obtained at an axial distance of  $x/D = 10$ .

#### Discussion and Concluding Remarks

The work reported here supports the concept according to which mixing layers have basic structures which consist essentially of arrays of relatively large vortices or eddies, moving downstream, but keeping their identity for fairly long periods. The term 'coherent structures' has been coined for these eddies. The present data have shown that this type of large scale structure can be detected in jet flames and that the ionisation probes with their high frequency response, can be used to derive the spectra and space-time cross-correlations required for the investigation of these structures, rather analogous to the use of hot wires in cold jets. This is because the reaction zones, which the ionisation probes detect, are strongly interrelated with the larger eddies, both in their spatial distributions and their convective properties.

Conditional sampling techniques<sup>11, 12</sup> have shown that the two interfaces on either side of the cold mixing layers, behave rather independently of each other. However, as has been discussed on the basis of earlier data,<sup>1</sup> the 'double structure' noted in the present jet flame mixing layer, appears to have a different source than these cold jet observations. The slow moving outer, large eddies appear to result from a separate instability mechanism than the rather smaller, faster moving eddies on the inner side of the mixing

layer.

Recent models<sup>13, 14</sup> for mixing layers without heat release, have been based upon an axial array of similar vortices or large eddies, being convected downstream. This provides some clarification on the entrainment and mixing mechanisms: the leading edge of the eddy induces an outward flow of potential core fluid, while the trailing edge entrains fluid from the outer low velocity region.

The two streams are engulfed by the eddy, within which rapid micromixing occurs. Yule<sup>15</sup> proposed that for such a situation in the combustion case, reaction would occur primarily in relatively narrow regions near the outer edges of the eddies, where stoichiometric conditions existed. Thus reaction zone structures and movements should provide information on the eddy structures with which they are associated. The present data clearly support this proposal, with the added complication of the possible coexistence of two distinct eddy types at any axial station, depending upon the equivalence ratio and  $Re$  of the fuel jet. It is important to note that the bulk of the data reported here are for transitional jet flames, i.e. for regions near the burner where the stabilizing force of viscosity is important. This region has been chosen for initial study, firstly, because it is an ideal situation for the development of instrumentation techniques and physical models and, secondly, for direct comparison with the predictions of time stepping computer models. However it has been described<sup>1</sup> how large coherent eddies can be detected for the full flame length, albeit increasing in complexity as they move downstream. The effects of combustion on the mixing layer include changes in the initial instability characteristics, increase in gas viscosity with increase in temperature and flow changes due to expansion. Some of these effects have been reported and the most obvious result, found for velocity measurements<sup>1</sup> in a flame with  $Re = 10^4$  and  $\phi = 10.4$  and in non-burning flow with the same Reynolds number, showed that the potential core in cold flow disappears at  $x/D \approx 4$ , while in the flame it was still present at  $x/D = 20$ . This shows

the strong influence of combustion on the mixing characteristics of the jet. The same observation can be made regarding the velocity profiles shown in Figure 1 for all of the flames studied here. Figure 1 also clearly demonstrates the 'humps' and inflexion points found in the flames, but not in the cold jets. These humps are likely to be related to the double vortex structure of the flame mixing layers. This double structure is confirmed by the ionisation probe measurements, including both the spectra and correlations of ion current signal. As shown by Figure 3, for the lowest equivalence ratio, when the region of stoichiometry (and thus the main reaction zone) is near the mixing layer centre, the signals are most strongly affected by the lower frequency vortices. When the measuring point is nearer the inner interface, or for higher  $Re$  and higher  $\phi$ , the influence of the higher velocity, higher frequency, structures is evident. A small positive shift was observed (Fig. 4) with increasing Reynolds number, in the low frequency peaks in the spectra of flames with the same equivalence ratio. This is in qualitative agreement with what one would expect for the Kelvin-Helmholtz instabilities in the cold jet case.

From the measurements presented in Figure 5, it appears that the average, large vortex, passing frequency at  $r/D = 0.5$  as detected by the ionisation probe (corresponding to the reciprocal of the delay time from the origin to the second peak in the auto-correlogram) is relatively constant. On the other hand, the average convection velocity of these vortices (obtained from cross-correlation measurements in the same flame and radial position) increases almost linearly with axial distance (Fig. 9). We may conclude that the scale of the vortices increases proportionally to convection velocity. This increase is likely to be attributable to dilatation accompanying heat release although a contribution from buoyancy forces is also present. There is also photographic evidence of movement of the eddies inwards, towards the jet flame centre, which should also be accompanied by acceleration.

From the profiles of flow velocity and convection velocity at the same axial station (Fig. 10), it may be noticed that the latter is almost constant across the mixing layer, and its value is  $0.3 \leq U_c/U_J \leq 0.45$  for the regions and flames studied. This is significantly less than the value  $U_J/U_c \approx 0.6$  found for large eddies in cold jets and it is again indicative of the influence of the outer vortices in the flame and their dominating contributions to the ionisation probe signals.

It is interesting to note that the inner, high frequency, vortices can be detected in the cross-correlations for certain flames and their convection velocities (with  $U_c/U_J \approx 0.85 U_J$ ) are in good agreement with those measured from ciné films. These observations are consistent with one of the classical concepts of turbulence by which large eddies induce convection velocities which are relatively constant across the flow, and significantly different from local mean particle velocities, whilst small eddies tend to be convected at close to the local mean velocity. If one assumes that the establishment of the 'turbulent shapes' of auto-correlations is a reasonable indication of the establishment of turbulent flow, data such as that shown in Figure 5 can be used to estimate the length of the flame transition regions  $x_T$ . It is interesting to note that in general  $x_T$  does not increase between the cold and jet flame cases, to the same extent as the observed increase in the jet potential core length. For example, for the flow with  $Re = 10^4$  and  $\phi = 2.62$ ,  $x_T$  increases from 4D to 12D between the cold jet and jet flame cases; while the jet potential core length increases from 4D to 24D approximately.

The above represents a selection of data which is intended to show the usefulness of the multiple-ionisation probe technique for the examination of flame structure, when combined with statistical data analysis techniques with variation in spatial separation and time delay. In addition to information on local reaction rates, the technique provides data on eddy size, eddy

convection, eddy interaction, transition, periodicity etc. For a full appreciation of the flame structure using this technique, extensive supporting data, using other measurement techniques, are required. This is beyond the scope of the relatively restricted length of the present paper; but it is worthwhile to note that such data have, and are continuing to be, derived by the authors, for example by using temperature, velocity and ionisation probes simultaneously to gain more detailed information on eddy structure. It must also be emphasised that although these results are of interest in their own right, the ultimate overall objective of the authors'<sup>1</sup> research is to provide data which are of fundamental use in the development of flow models developed in parallel; hence the systematic variation in initial flow conditions and the simple and carefully controlled initial conditions. Finally the great importance of the larger scales of motion in the flames, both transitional and turbulent, should again be emphasised on the basis of the large bulk of data now gathered in these flames by the authors.<sup>1, 8, 12</sup> We are convinced that physically realistic turbulent combustion models must include some of the effects attributable to these relatively repetitive, strong and coherent eddies which appear to be a common, if not universal feature of transitional and turbulent shear flow.

#### Acknowledgements

The research reported in this paper is supported by the U.S. Air Force (AFOSR), U.S. Office of Naval Research (SQUID) and the U.S. Army (European Office of Research).

References

1. Yule, A. J., Chigier, N. A., Ralph, S., Boulderstone, R. and Ventura, J., 'Combustion-Transition Interaction in a Jet Flame', AIAA Paper 80-0077 presented at AIAA 18th Aerospace Sciences Meeting, Pasadena, Jan. 14-16, 1980.
2. Calcote, H. F., Eighth Symposium (International) on Combustion, p. 184, Williams and Wilkins, 1960.
3. Karlovitz, B., Denniston, D. W. Jnr., Knapschaefer, D. H. and Wells, F. E., Fourth Symposium (International) on Combustion, p. 613, Williams and Wilkins, 1953.
4. Lockwood, F. C. and Odidi, A. O. O., Fifteenth Symposium (International) on Combustion, p. 561, The Combustion Institute, 1975.
5. Elgobashi, S. E. and Pun, W. M., Fifteenth Symposium (International) on Combustion, p. 1353, The Combustion Institute, 1975.
6. Suzuki, T., Hirano, T. and Tsuji, H., Seventeenth Symposium (International) on Combustion, p. 289, The Combustion Institute, 1979.
7. Smy, P. R., Advances in Physics, 25, 5, p. 517 (1976).
8. Chigier, N. A. and Yule, A. J., The Physical Structure of Turbulent Flames. Paper presented at the 17th Aerospace Sciences Meeting, AIAA, New Orleans, La., January 1979.
9. Clements, R. M. and Smy, P. R., J. Applied Physics, 41, p. 3745 (1970).
10. Chigier, N. A. and Yule, A. J., The Structure of Eddies in Turbulent Flames - I, Project SQUID Technical Report, March 1979.
11. Wagnansky, I. and Fiedler, H. E., J. Fluid Mechanics, 41, p. 327 (1970).
12. Yule, A. J., J. Fluid Mech., 89 (3), p. 413 (1978).
13. Fiedler, H. E., Turbulent mixing in non-reactive and reactive flows, S. N. B. Murthy (Ed.), p. 381, Plenum Press, 1975.
14. Lau, J. C. and Fisher, M. J., J. Fluid Mech., 67 (2), p. 299 (1975).
15. Yule, A. J., Chigier, N. A. and Thompson, D., Coherent Structures in Combustion, Symposium on Turbulent Shear Flows, Pennsylvania State University, 7, 41 (1977).

## Figures

- FIG. 1 Mean ion current and velocity profiles at axial distances  $x/D = 8$  and 16, for flames with equivalence ratio  $\phi = 2.62$ ; Reynolds number:  $\Delta$   $5 \times 10^3$ ,  $\square$   $10^4$ ,  $\circ$   $1.5 \times 10^4$ .
- FIG. 2 Signals from two ionisation probes in flame with  $Re = 10^4$  and  $\phi = 2.62$ . Radial position  $r/D = 0.5$ ; probe separation  $x = 10$  mm; axial (upstream) probe position: (A)  $x/D = 16.2$ , (B)  $x/D = 8.2$ . Lower traces correspond to upstream probe.
- FIG. 3 Power spectra of ion current at different longitudinal positions in two flames;  $Re = 10^4$ ,  $r/D = 0.5$ , equivalence ratios: (A)  $\phi = 2.62$ ; (B)  $\phi = 10.4$ .
- FIG. 4 Power spectra of ion current in flames with fixed equivalence ratio and variation in  $Re$ ;  $r/D = 0.5$ ,  $x/D = 4$ , equivalence ratio  $\phi = 2.62$ : (A)  $5 \times 10^3$ , (B)  $10^4$ , (C)  $1.5 \times 10^4$
- FIG. 5 Autocorrelations of ionisation probe signal for variation of distance downstream.  $Re = 10^4$ ;  $\phi = 2.62$ ;  $r/D = 0.5$ ;  $x/D$ : (A) 4.6, (B) 6.6, (C) 8.6, (D) 10.6, (E) 12.2.
- FIG. 6 Variation of periodicity of autocorrelation curve with downstream distance.  $Re = 10^4$ ;  $r/D = 0.5$ ; equivalence ratios:  $\Delta$ , 10.4;  $\circ$ , 2.62.
- FIG. 7 Cross-correlations with variation in streamwise probe separation.  $Re = 1.5 \times 10^4$ ;  $\phi = 2.62$ ;  $r/D = 0.5$ ; axial position (fixed probe)  $x/D = 4$ ; probe separation: (A) 5 mm; (B) 15 mm; (C) 30 mm; (D) 50 mm; (E) 80 mm.
- FIG. 8 Convection times from main peaks of cross-correlations;  $r/D = 0.5$ ; flame parameters:  $\square$   $Re = 10^4$ ,  $\phi = 2.62$ ;  $\circ$   $Re = 10^4$ ,  $\phi = 10.4$ ;  $\Delta$   $Re = 1.5 \times 10^4$ ,  $\phi = 2.62$ . Also convection times from 'high frequency peaks':  $\bullet$   $Re = 10^4$ ,  $\phi = 10.4$ ;  $\blacktriangle$   $Re = 1.5 \times 10^4$ ,  $\phi = 2.62$ .
- FIG. 9 Axial variation of convection velocity;  $r/D = 0.5$ ;  $Re = 10^4$   $\phi = 2.62$ ;  $\square$  from probes at fixed separation  $\Delta x = 10$  mm;  $\circ$  from probes with varying separation, fixed probe at  $x = 4D$ .
- FIG. 10 Velocity measured by laser anemometry ( $\square$ ) and convection velocity obtained from cross-correlation ( $\diamond$ ) at  $x/D = 10$  in a flame with  $Re = 10^4$  and  $\phi = 2.62$ .



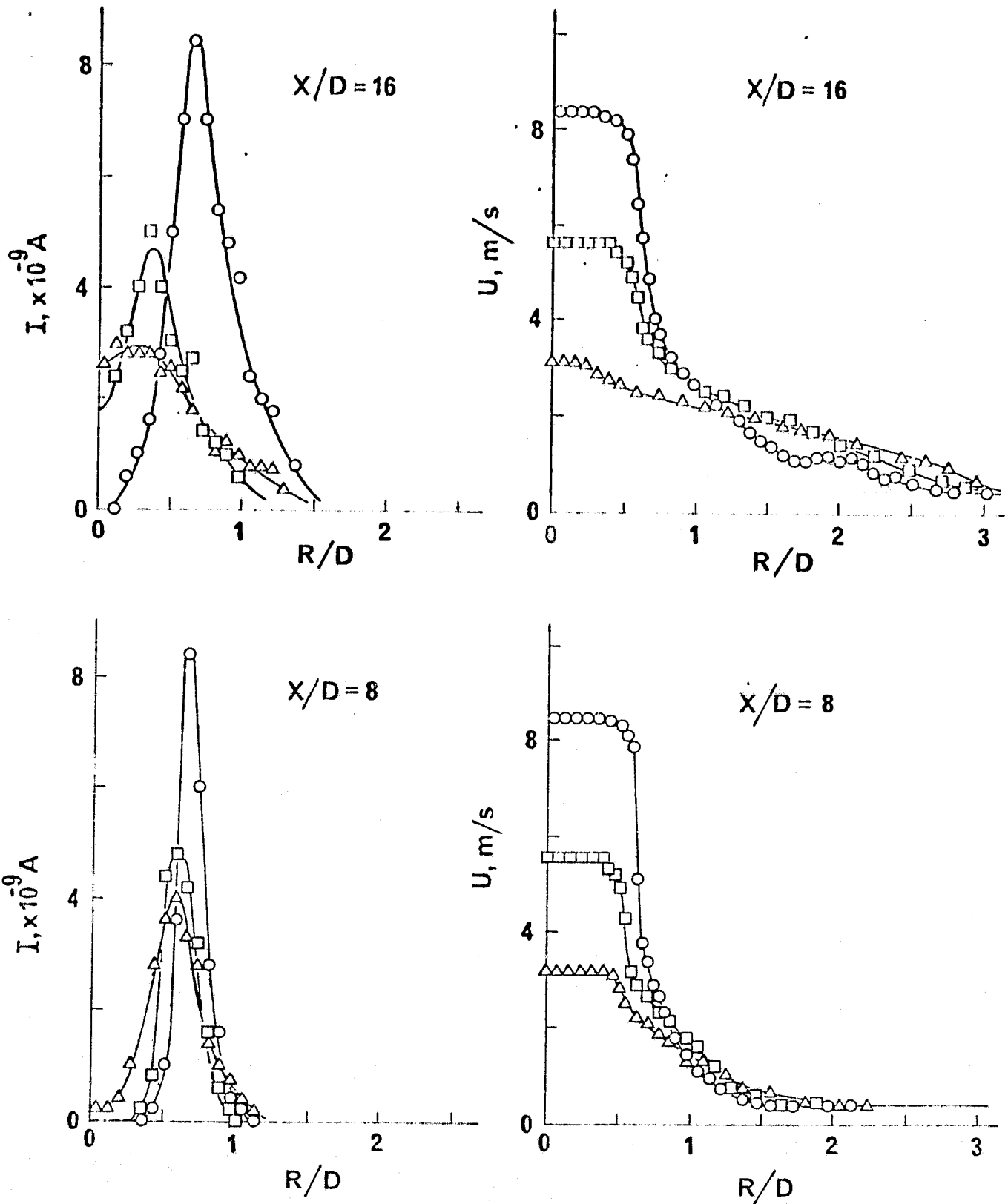


FIG. 1 Mean ion current and velocity profiles at axial distances  $x/D = 8$  and 16, for flames with equivalence ratio  $\phi = 2.62$ ; Reynolds number:  $\Delta$   $5 \times 10^3$ ,  $\square$   $10^4$ ,  $\circ$   $1.5 \times 10^4$ .

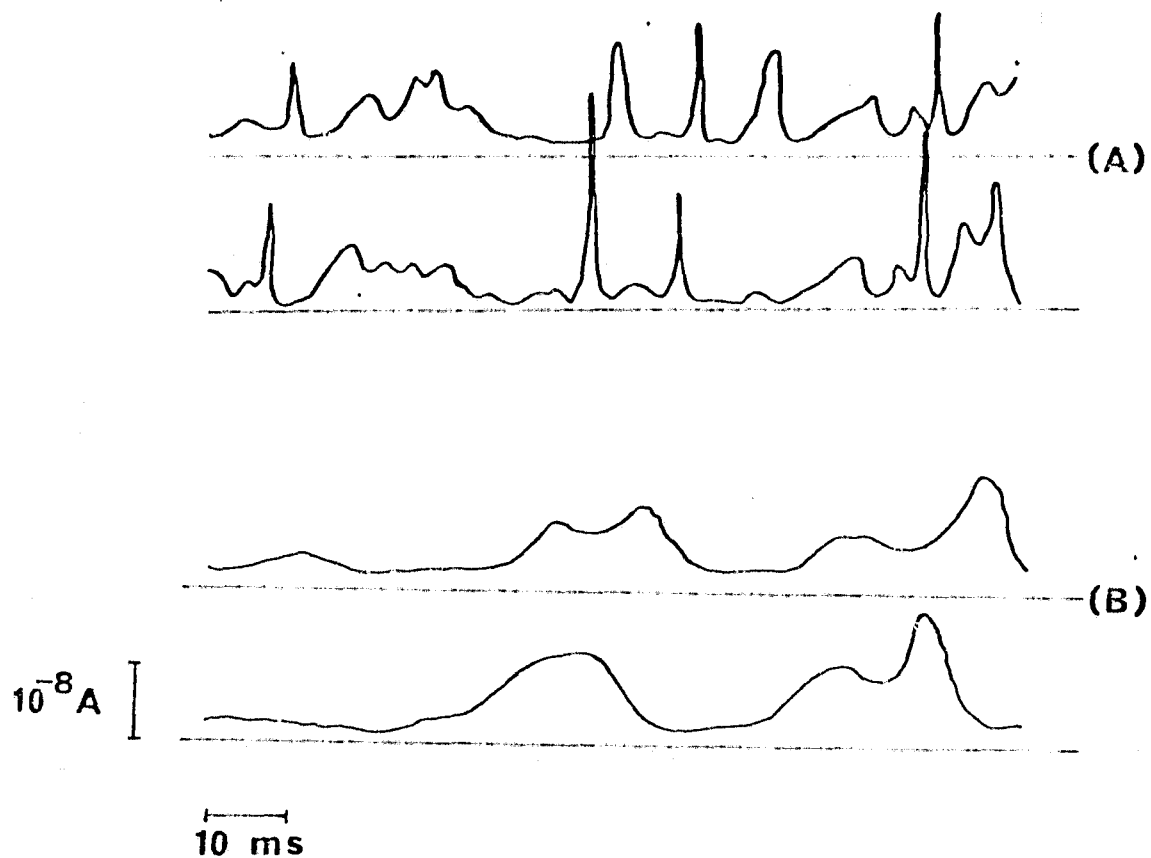


FIG. 2 Signals from two ionisation probes in flame with  $Re = 10^4$  and  $\phi = 2.62$ . Radial position  $r/D = 0.5$ ; probe separation  $x = 10$  mm; axial (upstream) probe position: (A)  $x/D = 16.2$ , (B)  $x/D = 8.2$ . Lower traces correspond to upstream probe.

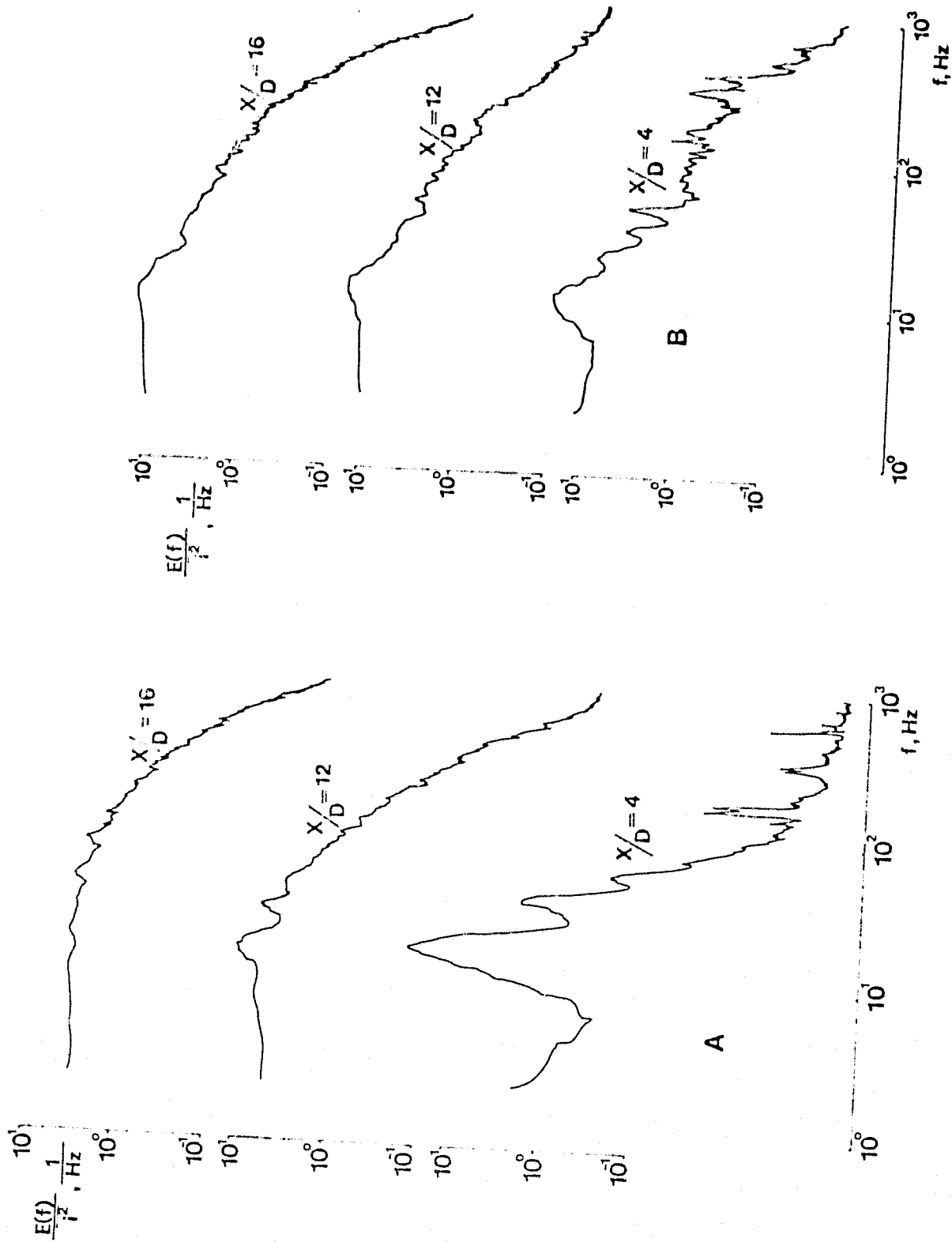


FIG. 3 Power spectra of ion current at different longitudinal positions in two flames;  $Re = 10^4$ ,  $r/D = 0.5$ , equivalence ratios: (A)  $\phi = 2.62$ ; (B)  $\phi = 10.4$ .

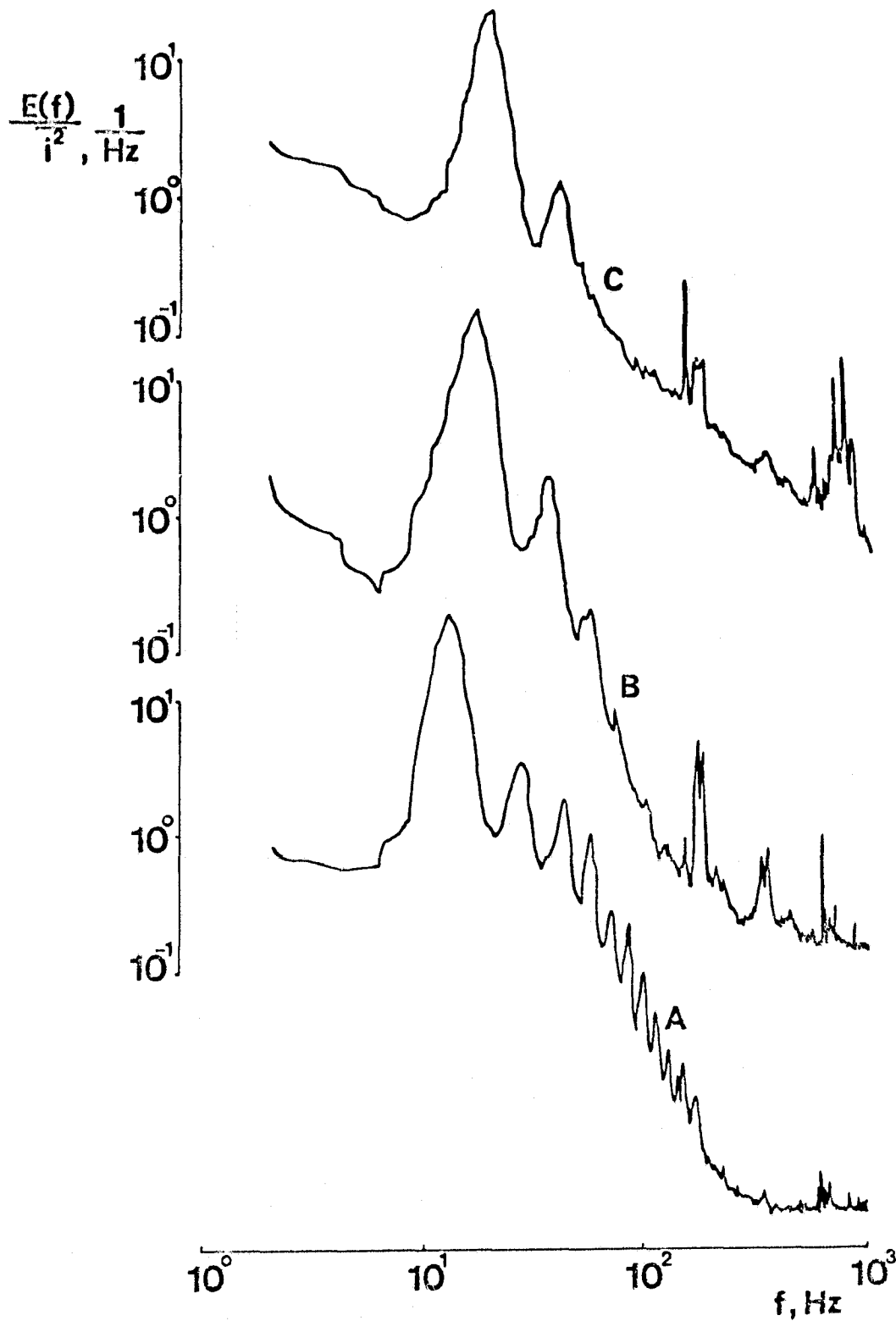


FIG. 4

Power spectra of ion current in flames with fixed equivalence ratio and variation in  $Re$ ;  $r/D = 0.5$ ,  $x/D = 4$ , equivalence ratio  $\phi = 2.62$ : (A)  $5 \times 10^3$ , (B)  $10^4$ , (C)  $1.5 \times 10^4$

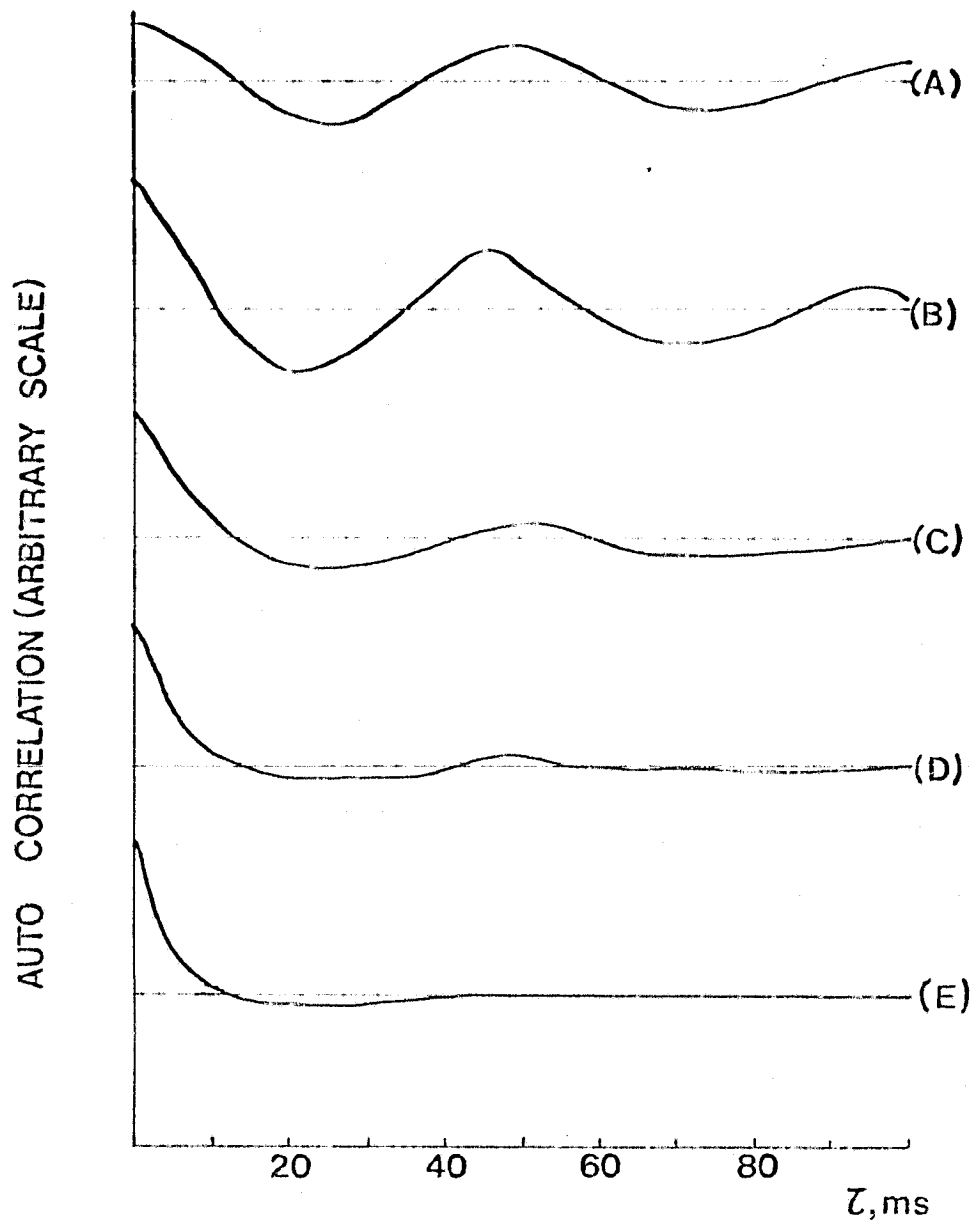


FIG. 5 Autocorrelations of ionisation probe signal for variation of distance downstream.  $Re = 10^4$ ;  $\phi = 2.62$ ;  $r/D = 0.5$ ;  $x/D$ : (A) 4.6, (B) 6.6, (C) 8.6, (D) 10.6, (E) 12.2.

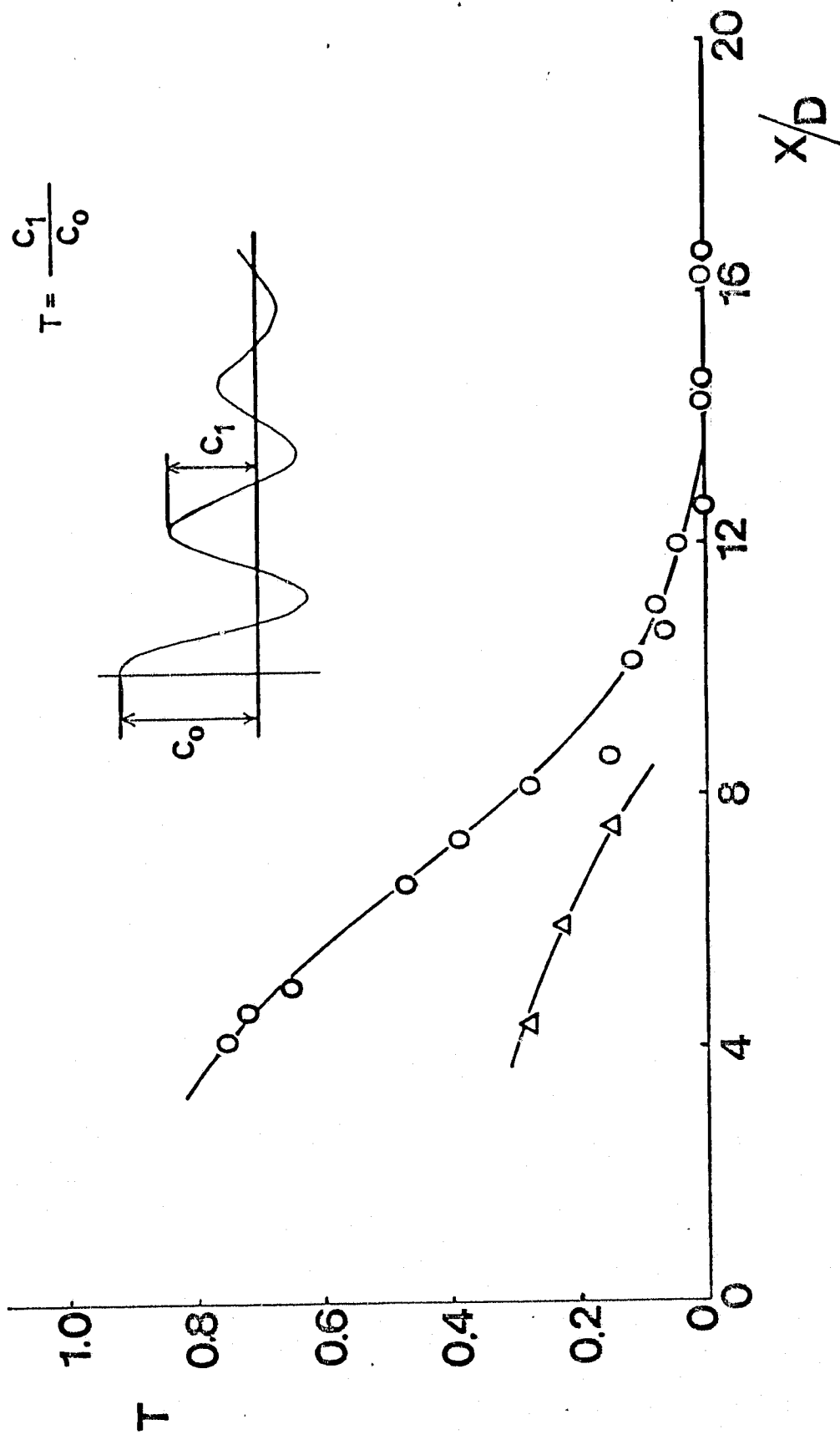


FIG. 6 Variation of periodicity of autocorrelation curve with downstream distance.  $Re = 10^4$ ;  $r/D = 0.5$ ; equivalence ratios:  $\Delta$ , 10.4;  $\circ$ , 2.62.

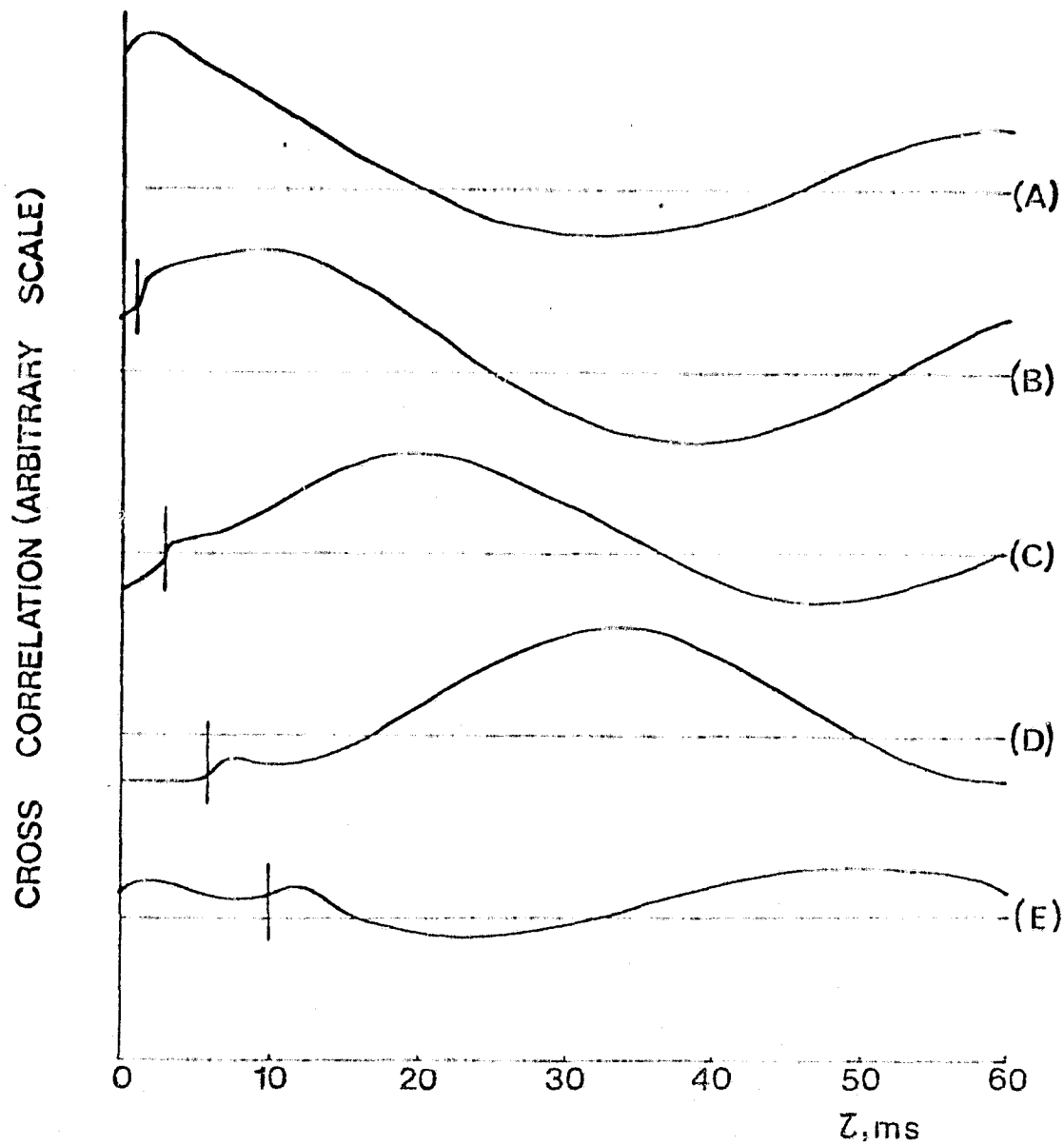


FIG. 7 Cross-correlations with variation in streamwise probe separation.  $Re = 1.5 \times 10^4$ ;  $\phi = 2.62$ ;  $r/D = 0.5$ ; axial position (fixed probe)  $x/D = 4$ ; probe separation: (A) 5 mm; (B) 15 mm; (C) 30 mm; (D) 50 mm; (E) 80 mm.

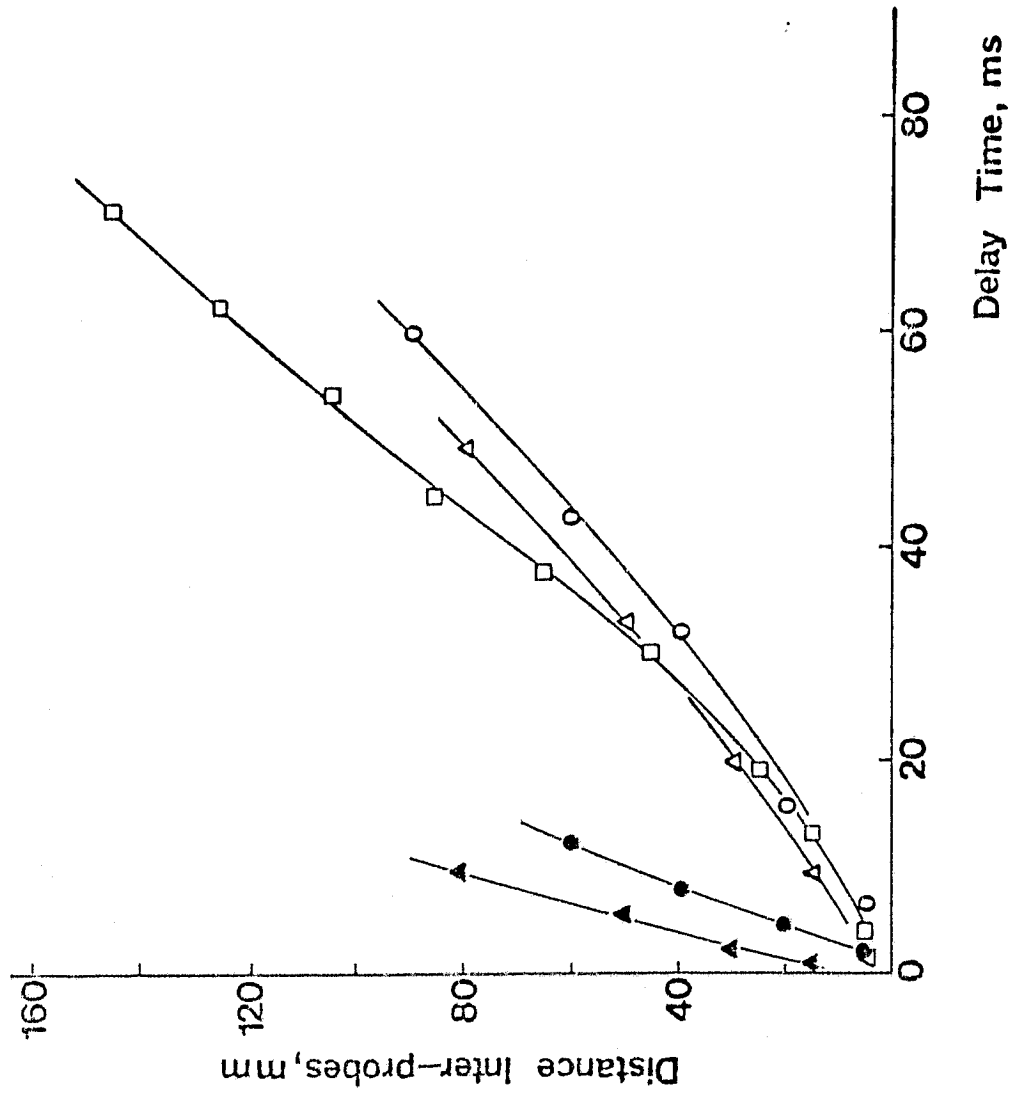


FIG. 8 Convection times from main peaks of cross-correlations;  $x/D = 0.5$ ; flame parameters:  $\square$   $Re = 10^4, \phi = 2.62$ ;  $\circ$   $Re = 10^4, \phi = 10.4$ ;  $\triangle$   $Re = 1.5 \times 10^4, \phi = 2.62$ . Also convection times from 'high frequency peaks':  $\bullet$   $Re = 10^4, \phi = 10.4$ ;  $\blacktriangle$   $Re = 1.5 \times 10^4, \phi = 2.62$ .



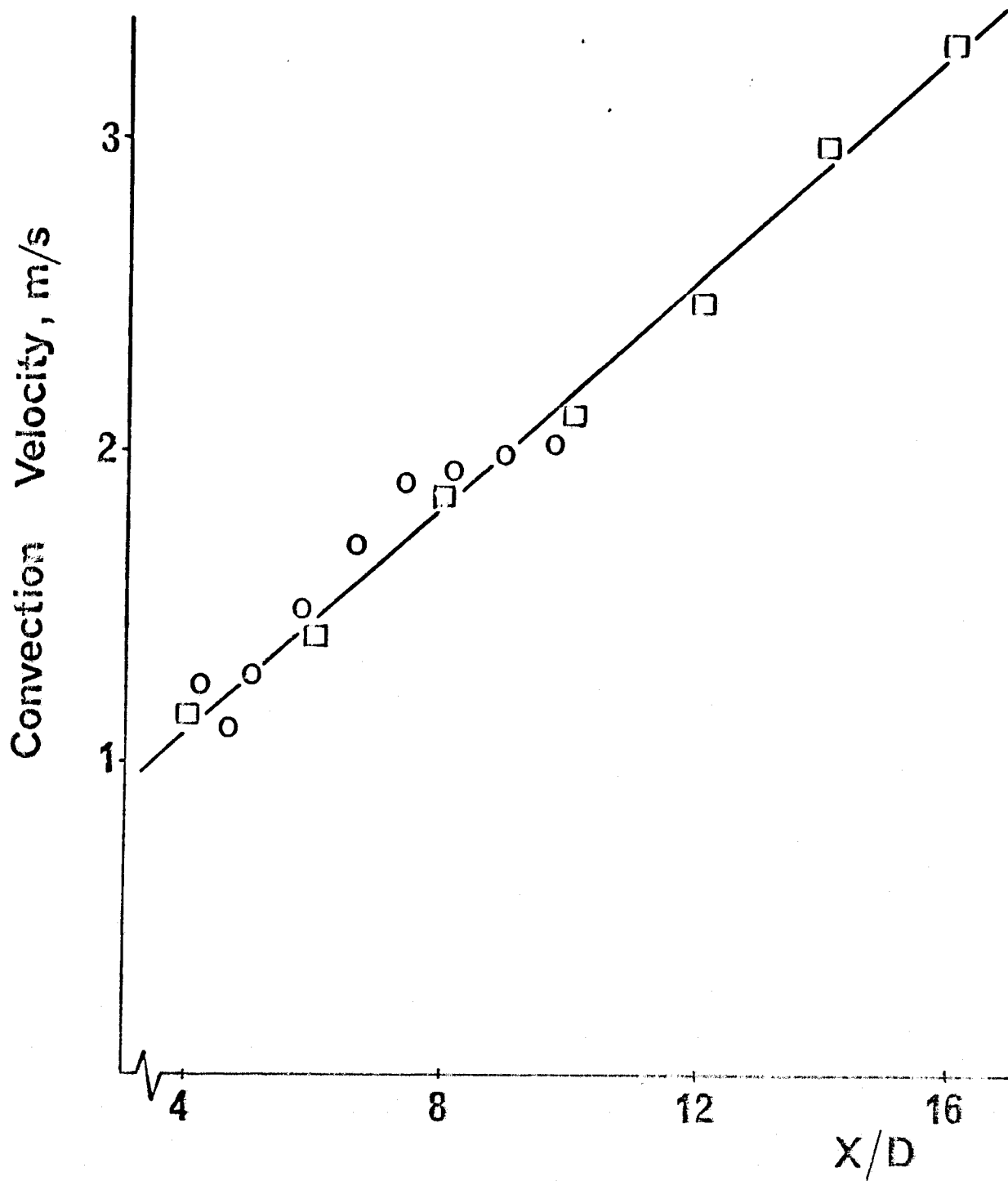


FIG. 9 Axial variation of convection velocity;  $r/D = 0.5$ ;  $Re = 10^4$   
 $\phi = 2.62$ ; □ from probes at fixed separation  $\Delta x = 10$  mm;  
 ○ from probes with varying separation, fixed probe at  $x = 4D$ .

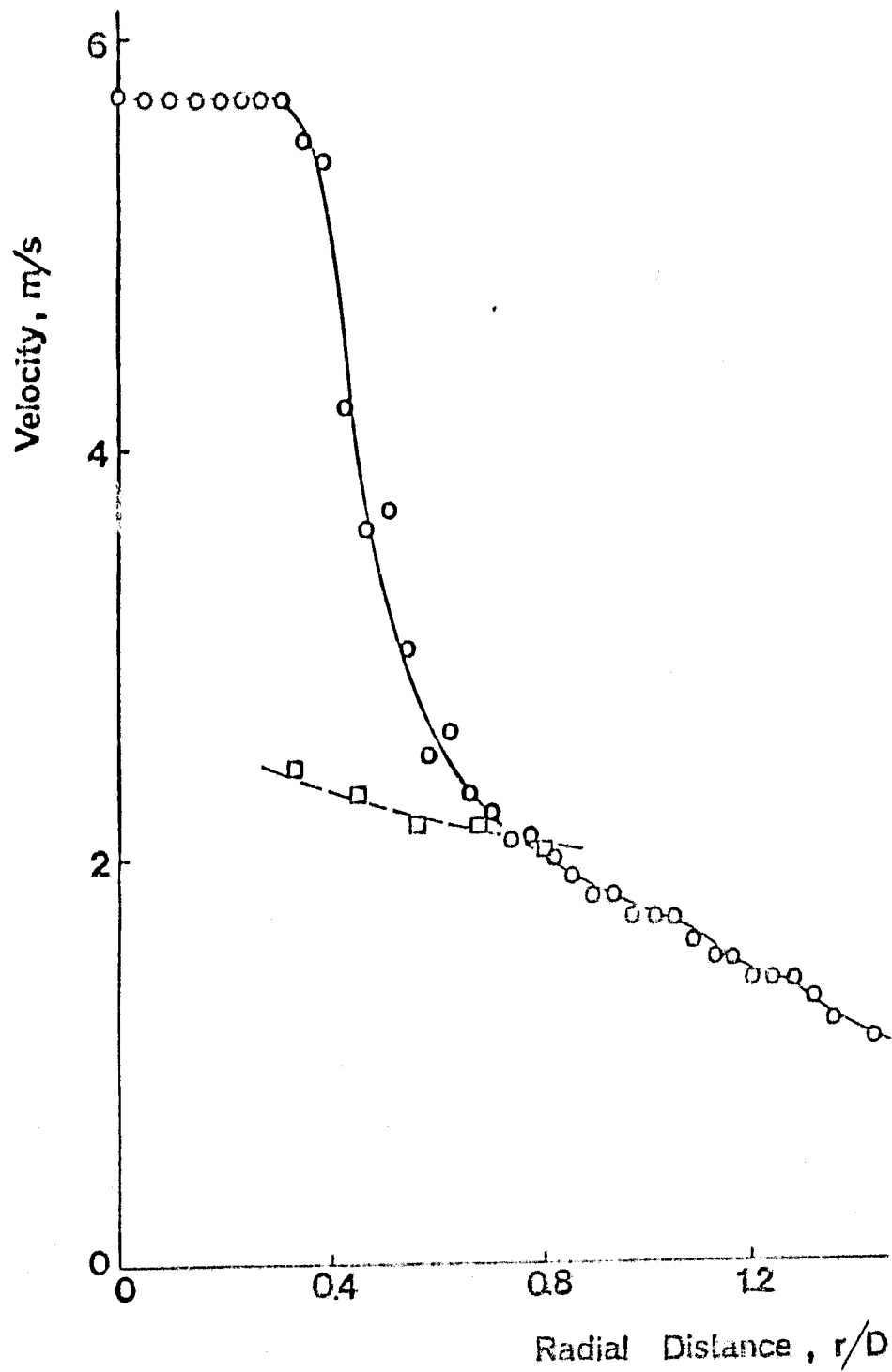


FIG. 10 Velocity measured by laser anemometry ( O ) and convection velocity obtained from cross-correlation ( □ ) at  $x/D = 10$  in a flame with  $Re = 10^4$  and  $\phi = 2.62$ .